Lens Heating Challenges for Negative Tone Develop Layers with Freeform Illumination: A comparative study of experimental vs. simulated results

Scott Halle[a*], Michael Crouse[b*], Aiqin Jiang[b], Youri van Dommelen[b], Tim Brunner[c]
Blandine Minghetti[d], Matt Colburn[a], Youping Zhang[e]

[a]IBM Research, Albany Nanotech 257 Fuller Road, Albany NY 12203 USA
[b]ASML 320 Ushers Road, Ballston Lake NY 12019 USA
[c]IBM Research, Semiconductor Research and Development Center 2070 Route 52, Hopewell Jct NY 12533 USA
[d]ASML 60 Merritt Bld, Fishkill NY 12524 USA
[e]ASML BRION 4211 Burton Drive, Santa Clara CA 95054 USA

ABSTRACT

Negative tone development (NTD) processes have been widely explored as a way to enhance the printability of dark field features such as contact holes and trenches. A key consequence of implementing NTD processes and subsequent tone reversal of dark field reticles is the significantly higher transmission of bright field masks and thus higher light intensity in the projection optics. This large increase in mask transmission coupled with the higher throughput requirements of multiple patterning and the use of freeform illumination created by source mask optimization creates a significant amount of lens heating induced aberrations that must be characterized and mitigated. In this paper, we examine the lens heating induced aberrations for high transmission reticles common to NTD using both simulations and experiments on a 193 immersion lithography tool. We observe a substantial amount of aberrations as described by even and odd order Zernike drifts during the course of a wafer exposure lot. These Zernike drifts per lot are demonstrated to have the following lithographic effects: critical dimension shifts, pitch dependent best focus shifts and image placement errors between coarse and fine patterned features. Lastly, mitigation strategies are demonstrated using various controllers and lens manipulators, including FlexWave with full Zernike control up to Z64, to substantially reduce the lens heating effects observed on-wafer.

Keywords: lens heating, NTD, ASCAL, lens aberrations, FlexWave

1. INTRODUCTION

1.1 Defining the Relationship Between NTD and Lens Heating

Tone reversal techniques have been investigated as a resolution enhancement strategy for dark field levels, particularly metal trenches and contact holes, for well over a decade.[1] However, recent advancements in using standard positive tone resists coupled with a solvent-based developer has allowed the superior performance of positive tone resists to be coupled with improved aerial image quality of a bright field mask.[2,4,6] This has resulted in a significant improvement in the lithographic performance of dark field layers and allowed continued scaling to meet the needs of sub-22 nm node designs. However, as with any new process technology, there are many components that must be assessed for it to be deemed viable for manufacturing. The confluence of three important effects has created a need to address lithographic lens heating concerns for these new negative tone development (NTD) processes. Those contributing effects are: higher scanner throughput for double patterning, more localized illumination energy from source mask optimization (SMO) freeform pupils and significantly higher reticle transmission as a product of the tone inversion.[5,7,8] This paper will examine the lens heating behavior

(* contact authors: S. Halle or M. Crouse)
S. Halle: email: halle@us.ibm.com
M. Crouse: email: michael.crouse@asml.com

Optical Microlithography XXV, edited by Will Conley, Proc. of SPIE Vol. 8326, 832607

of NTD processes with SMO and non-SMO pupils using both advanced lens heating simulation capabilities and experimental work. The goal of this work is threefold. Firstly, to predict the lens heating induced aberrations fitted to Zernike values for NTD SMO processes through both simulations using BRION's Lens Heating Module (LHM) and comparing to the experimental values by measuring the wavefront. Secondly, to simulate and measure the lithographic impact of lens heating induced aberrations for best focus shift, through slit CD fingerprint and image placement errors. Finally, we demonstrate mitigation strategies using a suite of controllers and lens actuators including new capabilities such as c-ASCAL (a computational feed forward calibration method) and FlexWave lens manipulator with expanded Zernike control up to Z64.

1.2 Lens Heating Concepts & Methodology

Lens heating is a concern in optical lithography because a small fraction of the light transmitted by the projection lens is absorbed to become heat. This heating profile of the lens is strongly influenced by illumination shape (or pupil) and the diffraction orders of the created by the patterns on the reticle. The energy flow through the lens is the convolution of the illumination and the mask diffraction orders creating localized temperature gradients that generate phase aberrations. The resulting aberrated wavefront is measured and fitted to the familiar Zernike fringe polynomials. The Zernike polynomials are well studied and have been classified into specific categories defined by their resulting effect on the transmitted image[3, 9, 10] . The symmetric Zernike orders are called even Zernike orders and typically impact the focus behavior of the aerial image. The asymmetric Zernike orders are called odd Zernike orders and typically impact image placement within the focal plane. Within these larger categories of even or odd Zernikes are subcategories that define specific aberration effects on the image such as H-V astigmatism (Z5), spherical (Z9) creating pitch-dependent focus shifts and coma (Z7) creating feature size dependent pattern placement errors.

A key element of this work is the predictive capabilities of lens heating simulation using BRION's Tachyon LHM that uses inputs of reticle design and process conditions to predict the lens heating induced aberrations fitted to Zernike terms. To understand the lithographic process implications of these Zernike drifts, we use LHM as described by Liu et al.,[11] and the companion lithographic simulator, Tachyon Lithography Manufacturability Check (LMC), to calculate best focus shifts, CD through slit fingerprint and image placement errors as a function of time and slit position due to lens heating.

The lens heating behavior is a strongly influenced by three parameters: illumination, reticle design and image size. Thus the experimental measurement of the aberrations can be used as a calibration to derive the scaling and time constants of the dynamic lens heating equation. There are four methods used in this work for collecting the experimental lens heating measurements through an exposure lot: 1.) Baseline lens heating lot with no corrections applied, 2.) No heating lot where only a small subset of dies are exposed per wafer with no corrections applied, 3.) Inline ASCAL lot, experimentally defined feed forward calibrations and 4.) c-ASCAL lot based on a simulated feed forward calibrations. The resulting time dependent wavefront measurements from the four types of lens heating lots are fitted to the relevant Zernike terms with both a time and slit position dependence The through slit behavior are described by the following terms: offset (Zx_0), tilt (Zx_1), curvature (Zx_2) and third-order (Zx_3). Now with the availability of FlexWave, and its extended performance range, the lens heating Zernike terms for reporting and mitigation have been extended from the prior cutoff of Z25 up to Z64. The values of Zernike drifts during a lens heating lot exposure can be reported in various ways. This work will report lens heating induced Zernike drifts across a 25 wafer lot exposure (starting from a cold state to ending in a hot state) or Zernike drift per lot (ZDPL) and for shorter timescales Zernike drift per wafer (ZDPW) which measures the change in aberration from start to finish of a single wafer exposure. This reporting methodology is most compatible with the measurements taken during the experiments (inline ASCAL). To reach a true saturation level can require multiple lens heating lots and the saturation point can be different, in terms of wafer count, for different experimental conditions.

The last component of lens heating mitigation strategy is the lens manipulator(s) that applies the corrections calculated by the controller. Advanced ASML immersion scanners have lens actuators that provide control of many different aberration modes. In addition to the default aberration control capability, the Advanced Lens Controller (ALC) option is available for greater dynamic range and can support the correction of new aberration types that commonly arise in advanced node development. The new FlexWave element is the next generation of

aberration mitigation by creating a tunable wavefront[12,14] and can support higher order aberration control up to Z64. In this work, we will present both experimental and simulated results using all three lens manipulators.

2. EXAMINATION OF LENS HEATING VARIABLES

The critical factors of lens heating for NTD processes are examined in the following discussion and the mitigation of these effects will be described in Section 3. The critical factors discussed here are: change in reticle transmission, effect of pupil shape, effect of pupil fill factor and impact of freeform SMO pupils. Additionally, the impact of odd order Zernikes, such as coma tilt (Z7_1) or 3-foil tilt (Z10_1) on image placement errors will be examined both with simulation and experiments to show that while the magnitude of odd order Zernikes typically created by lens heating is much smaller than corresponding even order Zernikes, the aberration sensitivities can be much higher. Thus, creating the case where relatively small odd order Zernikes coefficients can have a disproportionate lithographic impact to the features of interest.

2.1 Impact of Reticle Transmission

One of the most significant implications of NTD processes is the large change of reticle transmission from dark field to bright field for masks. The NTD tone inversion will convert a dark tone contact hole reticle with 10% transmission to a bright field version with a transmission approaching 90%. While it is not common for both tones to use equivalent doses, the power increase with reticle transmission is typically the dominate term and the transmitted power through the projection lens for NTD processes can increase significantly. It was typical for the high transmission masks used in this work to measure average power (at wafer level) in the range of 1 Watt during the experiments for nominal NTD processes. This is well within the range which where lens heating effects are known to become significant. Changes in reticle transmission typically result in proportional changes in the lens heating induced aberrations. Figures 1 and 2 show the simulated even and odd Zernike drift for a lens heating lot using a dipole 35x illumination for two reticles of similar design but different tones. The bright field reticle had a high 78% transmission (HT) and a lower medium field transmission field (MT) version measured 55% transmission. Overall the Zernike coefficients are observed to scale 21% due to a 29% reticle transmission change, with even order terms scaling 24% on average and odd order terms scaling slightly less at 20.0%. The third reticle (L-R 42% ave) in this chart is a dual tone reticle with the left side as bright field (78% transmission) and right side as dark field (5% transmission). Most of the Zernike terms increase linearly with the average reticle transmission as expected. However, the coma tilt aberration (Z7_1) increases by a factor of 2 for this L-R reticle. While this is an exaggerated case used only for a test reticle, it does illustrate the point that mixing different tones on a reticle can create a more complex lens heating response in general and larger specific lens heating concerns such as coma tilt (Z7_1). Therefore, the increase in reticle transmission created by tone reversal in NTD processes can have a significant impact on the lens heating behavior and ultimately affecting the on-wafer imaging performance.

2.2 Impact of Pupil Shape

The impact of pupil shape on lens heating induced aberrations is not as intuitive as the above section on reticle transmission. The energy distribution in the pupil from the illuminator must first be convolved with the diffraction orders from the reticle to create the diffraction pattern. It is the diffraction pattern that describes the angular distribution of energy absorption in the projection lens and defines the heating effects. An example of the impact of pupil shape can be examined with standard pupils using the same reticle: dipole, quasar and c-quad as shown in Figure 3 (even Zernike orders) and Figure 4 (odd Zernike orders). Note, as shown in Table 1, the pupil fill and the center value for partial coherence is held constant in the first three illuminations. The dipole 53x setting has both a larger dipole angle and therefore a 50% greater pupil fill than the dipole 35x. In this section, this is considered a shape effect because the larger dipole angle is primary cause for the different lens heating behavior. Figure 3 demonstrates the even Zernike orders show the expected effect that dipole strongly influences astigmatism (Z5, Z12 & Z21). Also expected is that quasar and c-quad pupils with rotational symmetry create significant amounts of spherical (Z9) and 4-foil aberrations (Z17) . However, the sizable amounts of odd order Zernike terms shown in Figure 4 are a bit of a surprise for some of the pupils. Specifically, the two rotationally symmetric pupils of quasar & c-quad create a significant amount of 3-foil tilt (Z10_1) and rotated 3-foil offset

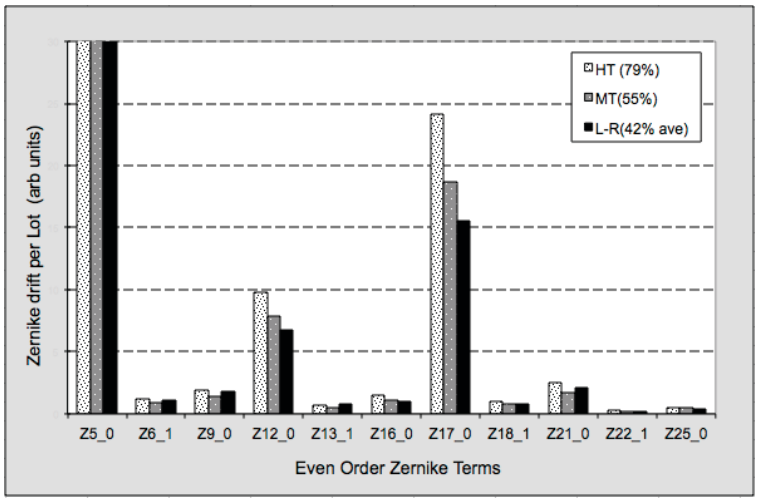

Figure 1. Simulated even order Zernike drift per lot for three reticle transmission values with similar design. Note that scaling factor is $7x$ odd Zernike orders.

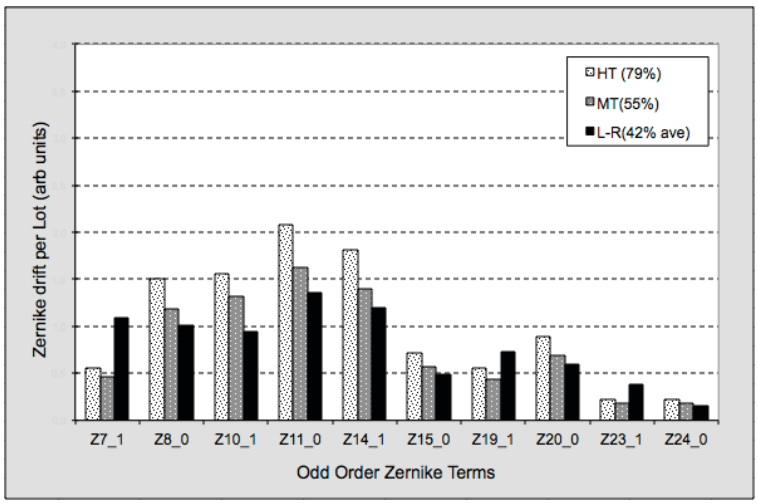

Figure 2. Simulated odd order Zernike drift per lot for three reticle transmission values with similar design. Note that scaling factor is $^1/_7th$ of even Zernike orders.

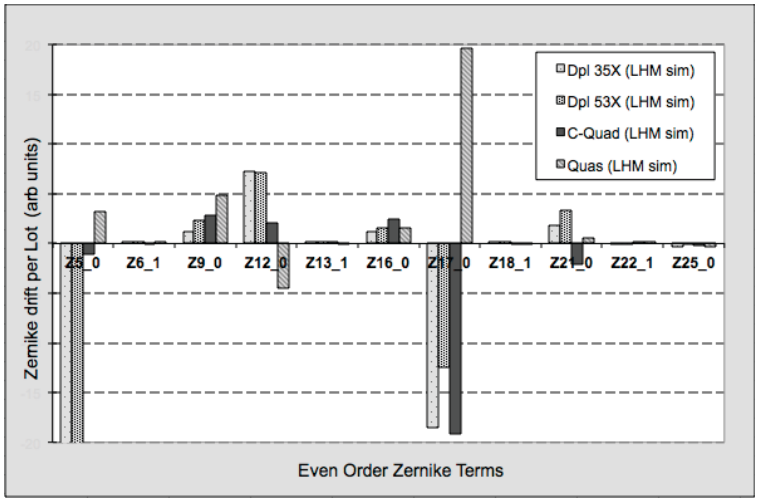

Figure 3. Simulated impact of pupil shape on even order Zernike orders. Note that scaling factor is $4x$ odd Zernike orders.

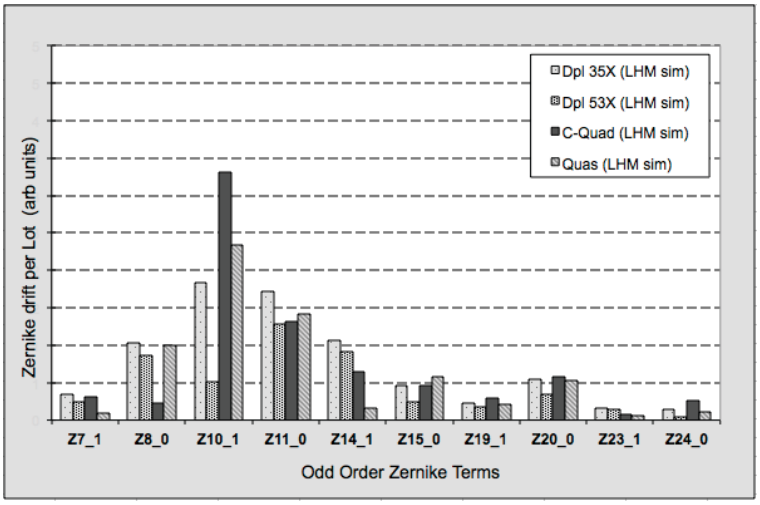

Figure 4. Simulated impact of pupil shape on odd order Zernike orders. Note that scaling factor is $^1/_4th$ of even Zernike orders.

(Z11_0). In contrast, dipole pupils are known to create odd order aberrations due to the breakdown of rotational symmetry. The lithographic effect of 3-foil aberration is image placement shift. The aberration sensitivity for 3-foil (Z10_1) and coma (Z7_1) will be shown in subsequent sections to be significant and can impact overlay budgets on-wafer.

Table 1. Comparison of standard pupil shapes.

Pupil Shape	Blade Angle	Inner Sigma	Outer Sigma	Fill Fraction	Symmetry
C-Quad	18	0.75	0.97	0.07	Rotational
Quasar	18	0.75	0.97	0.07	Rotational
dipole X	35	0.75	0.97	0.07	Nonrotational
dipole X	53	0.75	0.97	0.12	Nonrotational

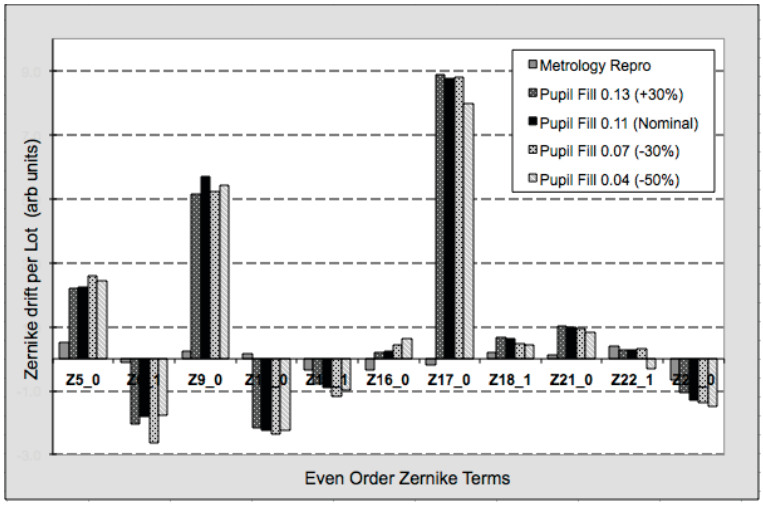

Figure 5. Experimentally measured impact of quasar pupil fill on even order Zernikes drift through lot exposure. Note that scaling factor is $4x$ odd Zernike orders.

2.3 Impact of Pupil Fill

In addition to the pupil shape, the pupil fill fraction is often considered an important parameter. As with the prior discussion on pupil shapes, the impact of pupil fill is also not intuitive. General guidelines for minimum pupil fill for scanners serve the purpose of protecting the optics and do not necessarily indicate the severity of lens heating behavior or the impact to the lithographic features of interest. An example of the impact of pupil fill only is given in Figures 5 and 6 with the experimentally measured lens heating behavior of four similar quasar pupils. The details of the pupils are given in Table 2. The nominal quasar pupil shown in the table meets the minimum pupil fill guidelines of 0.10 pupil fill fraction. The other three pupils are +30%, -30% and -50% scaling of the pupil fill keeping the center sigma and the quasar angle unchanged. This range of pupil fill spans a 70% change in the fill fraction with the largest fill of 0.13 (+30%) to the smallest fill fraction 0.04 (-50%). Thus we expected to observe a significant difference in lens heating induced Zernike drift per lot among these four quasar pupils. However, its is clear from Figures 5 and 6 that there is a negligible difference in both the even and odd Zernike values as simulated at wafer 25 (hot state). Therefore, pupil fill fraction is not a sufficient criterion to use when ranking candidate SMO pupils without further analysis through lens heating simulations and aberration sensitivities of the features of interest.

Table 2. Pupil fill impact using quasar illuminations.

Condition #	Sigma Inner	Sigma Outer	Fill Fraction	% Change
1	0.67	0.93	0.14	+30%
2	0.70	0.90	0.11	(nominal)
3	0.73	0.87	0.07	-30%
4	0.76	0.84	0.04	-50%

2.4 Examining SMO pupils

In this section we study the lens heating behavior of SMO freeform pupils and compare the experimentally measured behavior to the predicted results using Tachyon LHM. Figures 7 and 8 show both the experimentally measured and the simulated lens heating induced Zernike drift per lot for three different pupils with parameters given in Table 3 using the same high transmission reticle. Figure 7 shows the experimentally measured even Zernike orders impacting CD and focus while Figure 8 shows the experimentally measured odd Zernike orders which impact pattern placement. A couple of key observations can be drawn from these charts of the Zernike drifts per lot. The first observation agrees with the prior discussion that pupil shape has a significant impact

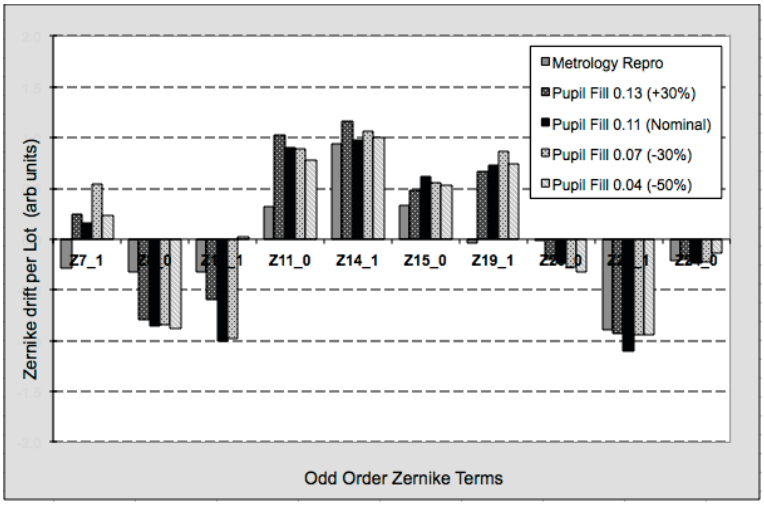

Figure 6. Experimentally measured impact of quasar pupil fill on odd order Zernikes drift through lot exposure. Note that scaling factor is $^1/_4 th$ even Zernike orders.

on the resulting lens heating aberrations. Notice the significant change in sign in astigmatism (Z5_0) and 4-foil (Z17_0) between SMO pupil #1 and SMO pupil#2. For this high transmission reticle (78%), we show a strong pupil-dependent lens heating signature, which is dominated by zeroth order effects, for the even order aberrations. The implication of this finding is that during the source mask optimization, a list of candidate SMO pupils is typically generated and evaluated. These candidate SMO pupils can display widely varying lens heating signatures for the similar set of design features. The aberration sensitivities of the design will determine which of the candidate SMO pupils is optimal from a lens heating perspective. The second observation is the through-lot odd order Zernike drift for these rotationally symmetric SMO pupils, while not zero, are much smaller when compared to the even order terms. Additionally, there is much less variation observed in the odd order Zernike's from pupil to pupil. This data suggests for rotationally symmetric SMO sources, the odd order Zernike terms are not as pupil specific as the even orders during the SMO procedure. The lithographic impact of the even order Zernike terms for best focus shift and CD through slit signatures will be examined in Section 3.3. The impact of the odd order Zernike terms will be discussed in the next section.

Table 3. SMO and annular pupil details for lens heating impact.

SMO Pupil #1	SMO Pupil #2	Annular Pupil
		
Fill Fraction 0.14	Fill Fraction 0.11	Fill Fraction 0.20

2.5 Impact of Image Placement Errors due to Odd Order Zernikes

The lithographic impact of the odd order Zernike terms were studied using a specifically designed interlaced overlay target composed from a fine pattern and a coarse pattern which are exposed together in a single exposure and measured using standard overlay metrology. The image placement errors generated by the odd Zernike orders will cause a differential image shift between the fine patterns and the coarse patterns of the overlay target. This image placement error can be both simulated and measured experimentally as an overlay shift (DX for dipole 35x). In Figure 9, we show both the simulated and experimentally measured overlay values from a cold-to-hot

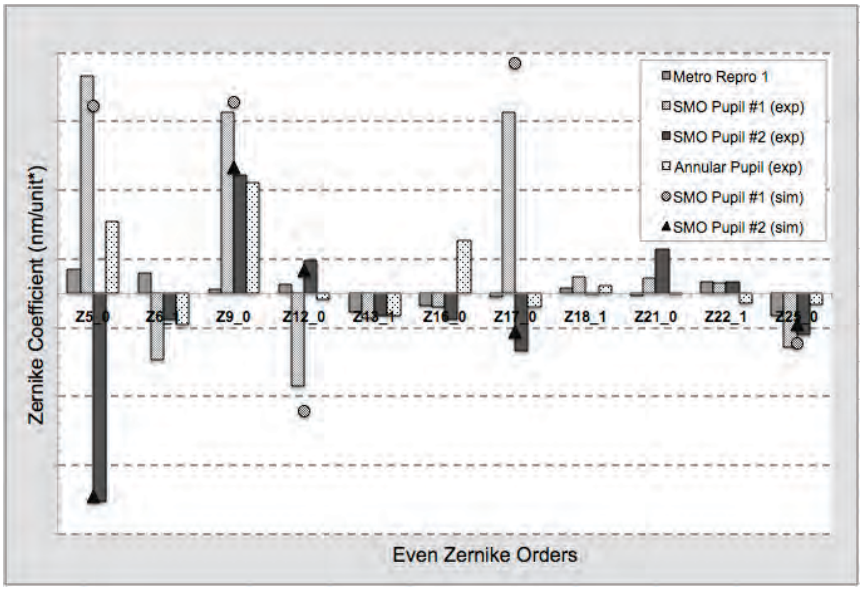

Figure 7. Experimentally measured SMO pupil impact on even order Zernike drifts per lot exposure. Note that scaling factor is $4x$ odd Zernike orders.

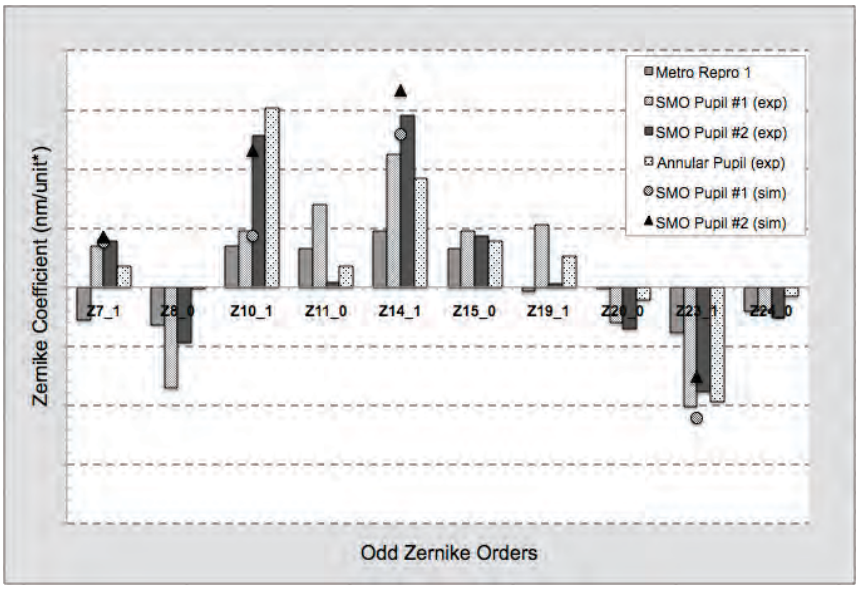

Figure 8. Experimentally measured SMO pupil impact on odd order Zernike drifts per lot exposure. Note that scaling factor is ${}^{1}/_{4}th$ even Zernike orders.

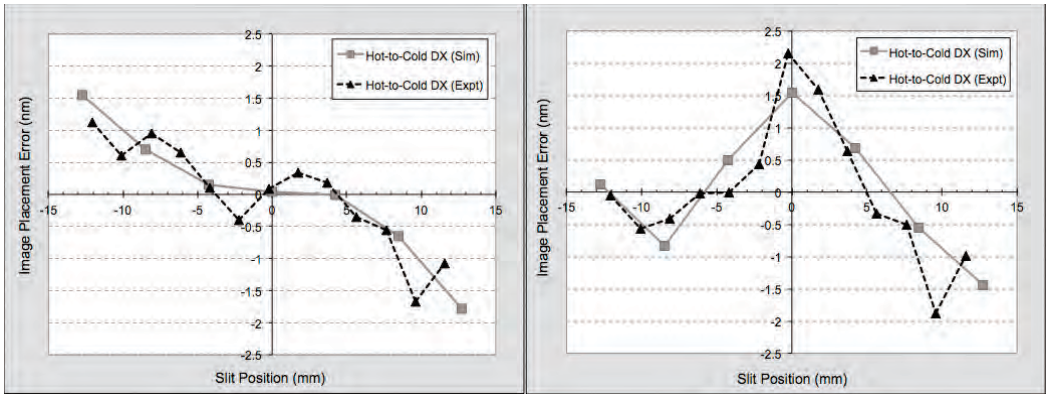

Figure 9. Comparing simulation and experiment for Cold-to-Hot Image Placement Errors using Medium transmission (on left) and Left-Right reticles (on right).

transition through an exposure lot using dipole 35x illumination. The left chart in Figure 9 shows the image placement error through slit for the overlay target on the medium transmission reticle. The right chart in Figure 9 shows the image placement error of the overlay target on the left-right combination reticle (left side is bright field, right side is dark field). The first observation is that the overlay measurements show a strong slit position dependence indicating the odd orders demonstrate the expected tilt through slit with small amount of higher order behavior for the medium transmission mask (left chart). Second observation is that the tone of the reticle has a strong impact on the direction of these tilts and the boundary between the two tones creates a peak in the image placement error at the center of the slit which does not occur when a single tone mask is examined. The final observation from Figure 9 is that these overlay effects through the slit are significant, on the order of 5 nm deviation through slit. Thus, the aberration sensitivities of the interlaced overlay targets must be examined and compared to product-like features to understand the impacts to overlay budgets.

Using Tachyon LHM & LMC, we computed the aberration sensitivities of the overlay target described above and compare it to a product-like feature (52 nm line & space) in Table 4. Thus, for every 1 nm of 3-foil (Z10) the image placement error will be 0.88 nm for the optical overlay target as compared to 0.37 nm shift for the product-like 52 nm line and space. This approximately 2x sensitivity can create the problem of overcorrecting the overlay for the lithographic features of interest based on measurements of the optical overlay target. This highlights one of the most important points of this work. Specifically, the smaller magnitudes of odd order Zernike terms cannot be neglected compared to the even Zernike orders due to the direct impact on image placement errors. Additionally, we have observed the odd orders Zernike terms are much less dependent on parameters such as pupil shape and fill fraction. Therefore, mitigation using a lens manipulator is the best means of controlling this type of lens heating effect vs. attempting to find a lens heating friendly SMO pupil.

Table 4. Simulated lens heating sensitivities of the optical overlay target and the product-like 52 nm line & space.

Aberration	Zernike term	Optical Ovl Target	52 nm Line & Space
coma	Z7	-0.69	0.14
3-foil	Z10	-0.88	-0.37
higher coma	Z14	-0.34	0.04

2.6 Kinetics of Lens Heating

In addition to the longer timescale of start-to-finish lot drift for aberrations, the dynamic behavior of lens heating within the lot is equally important to understand.[16] The dynamic behavior of the lens heating effect is described by each Zernike as a function of time during the exposure lot. Such behavior needs to be calibrated for each specific reticle design and pupil shape for the corresponding tool in order to achieve the best control performance. Figure 10 shows a portion of typical calibration curve for the SMO pupil #2 with the time dependent Zernike values normalized by the hot state (wafer 25) values. Note that the two dips in the calibration curves (time at

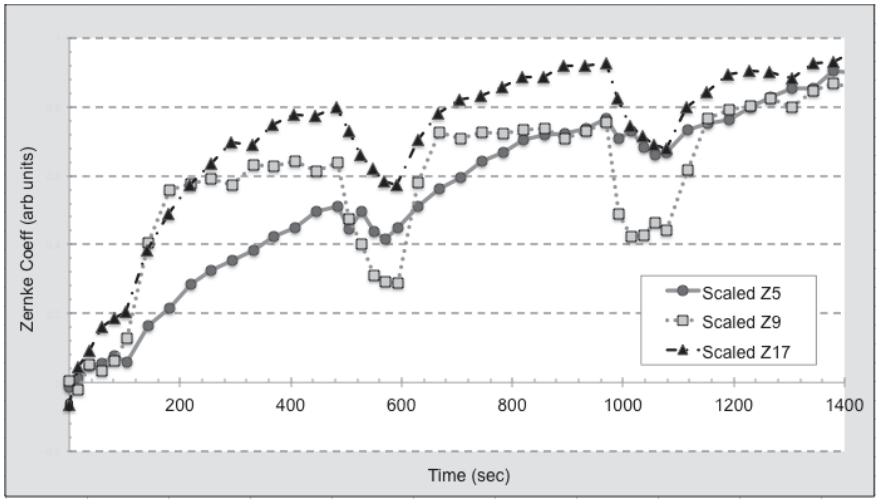

Figure 10. Experimentally measured dynamic lens heating behavior normalized by hot state Zernike values.

480 & 960 seconds) correspond to a cooling sequence used by the calibration for a more accurate numerical fit. Looking at the dynamic lens heating data in this way allows us to compare the time response of the different Zernike orders. It is clear from Figure 10, using the SMO pupil #2, that spherical aberration (Z9) has the fastest time response and astigmatism (Z5) has the slowest of the three Zernike orders examined. The implication of this finding is that if lens heating controls were not implemented, the effects of spherical aberration are more significant toward the early wafers in the lot while astigmatism effects will become more significant as the lot progresses depending on the process aberration sensitivities. An accurate lens heating calibration either experimentally using inline ASCAL or computationally using c-ASCAL will allow effective control of the dynamic lens heating behavior through the exposure lot.

3. LENS HEATING MITIGATION STRATEGIES

3.1 Defining Lens Heating Controls & Manipulators

The mitigation of lens heating effects requires an accurate calibration of the dynamic lens heating behavior, lens manipulators that correct different aberration modes, and a controller on the scanner that determines the corrections to be applied using the lens manipulators. There are various options when applying lens heating mitigation, meaning that either experimentally or simulated lens heating calibrations can be used by the controller to drive the various lens manipulators. The available lens manipulators that can be driven by the controller are: the default manipulators, the advanced lens controller (ALC) and the wavefront tunable FlexWave. The default lens manipulators are designed to handle the most common lens heating aberrations. The ALC option adds important capabilities for the following: rotated features typically used in DRAM designs, correction capability for asymmetric aberrations that impact overlay and additional correction for selected higher order aberrations that degrade the aerial image primarily by defocus. FlexWave is a new design in lens manipulators that allows for a programmable wavefront to be generated and supports higher resolution aberrations up to Z64.

3.2 Predicting & Measuring Mitigation Through Zernikes

The mitigation of lens heating aberrations can be demonstrated for various controller plus actuator schemes using Zernike drift per lot as the metric. Figure 11 shows the ZPDL for the key lens heating terms of Z5, Z9, Z12 & Z17 for the SMO pupil #1 and a combination of various controllers and actuators. The left most column of Figure 11 lists the description of the various mitigation schemes under each Zernike term. The two data columns of Figure 11 show the experimentally measured (left) or the simulated values (right) of the Zernike drift per lot. Note that blank entries in the tabular format of Figure 11 denote no data available, i.e. experiment was not run or the simulation was not possible. We can summarize the following four points from the data in Figure 11. Firstly, the measured experimental values and Tachyon LHM simulated values of the baseline heating case (with no controls applied) agree to within plus or minus (3σ) measurement error. Secondly, applying the lens heating control using the default lens manipulators significantly reduced the total aberration, with both the an experimental (inline ASCAL) and a computational (c-ASCAL) lens heating calibration. Thirdly, activating the ALC lens manipulator further reduces the aberration levels for Z9, Z12 and Z17. Finally, the simulated FlexWave lens manipulator, instead of ALC, gives the best response across all the aberrations shown here, particularly for the higher order ones such as 4-foil (Z17).

These promising simulated FlexWave results motivated further experimental investigation of FlexWave. The purpose of this experiment was to verify our prior simulations and experimentally demonstrate the capability of this new programmable wavefront actuator using both c-ASCAL and inline ASCAL for controlling through lot Zernike drifts. Figures 12 and 13 shows the through lot lens heating behavior for the three cases examined using dipole 35x illumination: 1.) Baseline with no heating corrections applied, 2.) FlexWave driven by c-ASCAL and 3.) FlexWave driven by Inline ASCAL. The Zernike drift per lot are lumped by classification (astigmatism, spherical, coma, etc.) for better comparison. The large astigmatism of the baseline lot dominates the lot drift behavior, but a measurable amount of 4-foil (Z17_0) is also present. Figure 12 shows that both c-ASCAL and inline ASCAL driven FlexWave reduce the large astigmatism (Z5) and 4-foil (Z7) drifts of the baseline case to below an acceptable threshold level. It is important to notice that the other aberration terms (coma, spherical, 3-foil) are not adversely impacted by FlexWave's correction of the astigmatism and 4-foil drift, thus demonstrating FlexWave's unique ability to selectively address specific Zernike terms without creating undesirable crosstalk. In order to better understand shorter time scale effects, we examined the Zernike drifts per wafer which is defined as the difference between the pre-exposure and post-exposure ILIAS measurement for each wafer in the lot. The Zernike drift per wafer values are averaged for all 25 wafers in the lot and the RMS Zernike values computed. The wafer-to-wafer variation of the Zernike amplitudes can be expressed as the Zernike drifts per wafer, which is shown in Figure 13 for the three experimental cases (baseline, c-ASCAL, inline ASCAL). Again, the baseline astigmatism is the dominate behavior also at the shorter wafer drift timescale, but the higher orders of 4-foil and 6-foil have become more important to control. Both the c-ASCAL and inline ASCAL driven FlexWave achieves an acceptable performance level for all Zernike terms at the wafer drift timescale as well as the previous lot drift timescale.

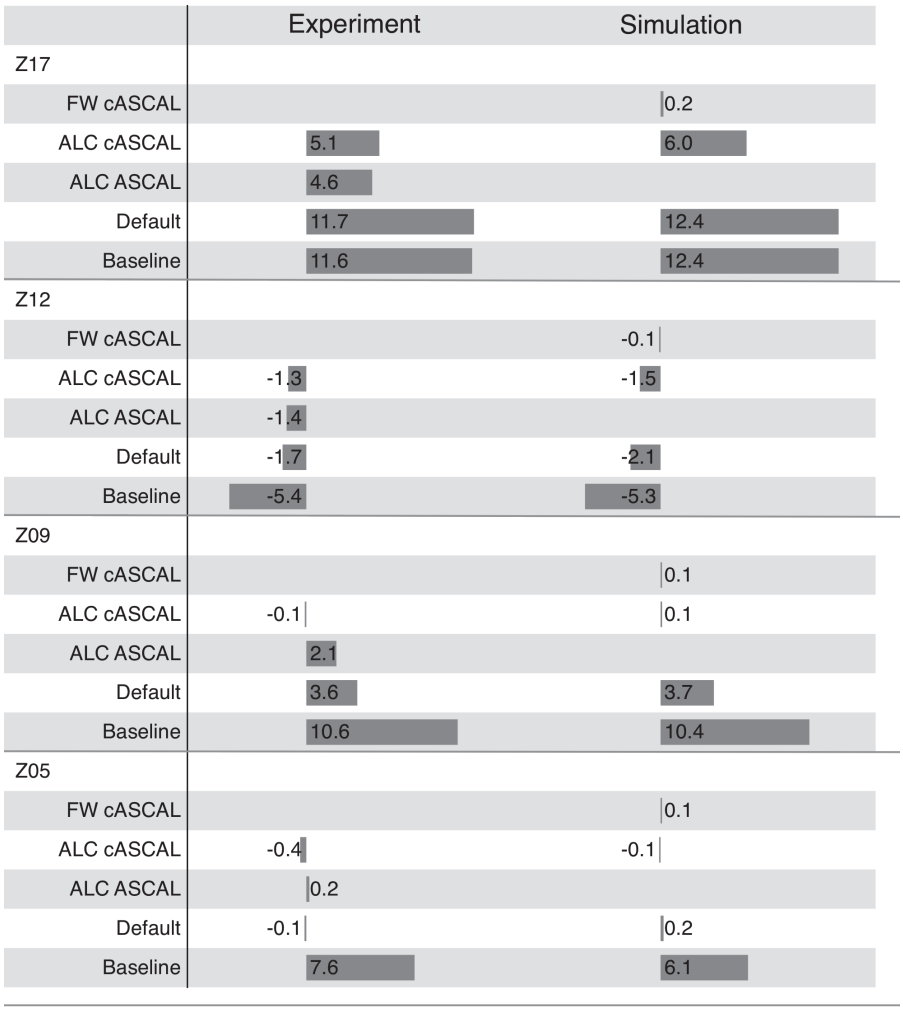

Figure 11. Simulated and experimentally measured residual Zernike drift per lot for typical lens heating aberrations demonstrating the effectiveness of various mitigation strategies. Illumination is SMO pupil #1 with the high transmission reticle.

Therefore, the lens heating induced aberrations reported as Zernike drift per lot and per wafer, can be simulated using Tachyon LHM and mitigated using a controller and a lens actuator with experimental verification. The default lens manipulator does a reasonable job of improving typical lens heating aberrations such as astigmatism (Z5_0) and spherical (Z9_0) but the addition of ALC expands the dynamic range and adds 4-foil correction capability. FlexWave, in comparison, shows superior correction capabilities for the entire range of aberrations with similar results achieved when driven both by Inline ASCAL or c-ASCAL. The next step in this analysis is to follow the lithographic impact on wafer as is described in the following section.

3.3 Through Lot Focus Control of Lithographic Features

One of the most important on-wafer effects for the dominant even order Zernike terms is pitch dependent shifting of best focus during a lot exposure as the lens heats. The FlexWave system with dipole 35x illuminator with the same high transmission reticle was used for this study. Specifically, four features were chosen for the analysis:

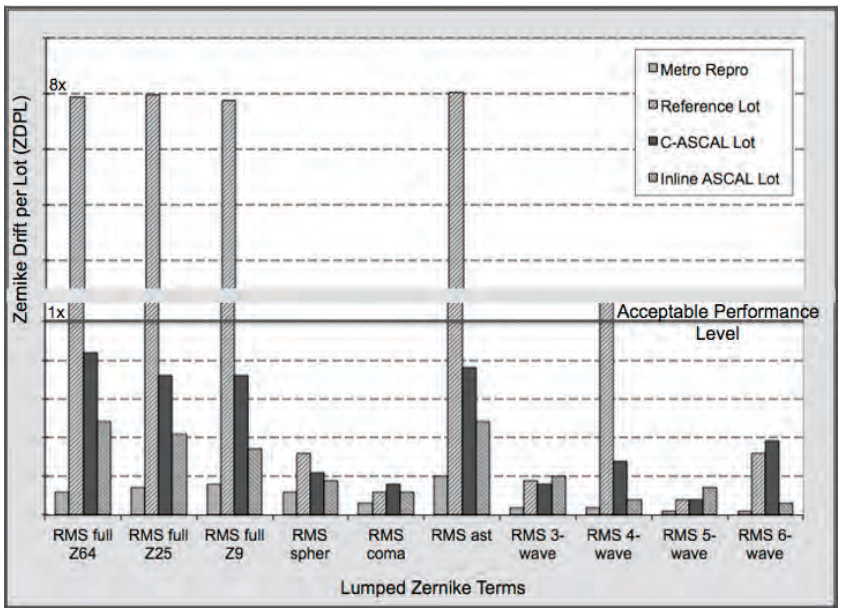

Figure 12. Experimentally measured Lot Drift for lens heating control lots with FlexWave comparing Inline ASCAL, C-ASCAL and the baseline performance.

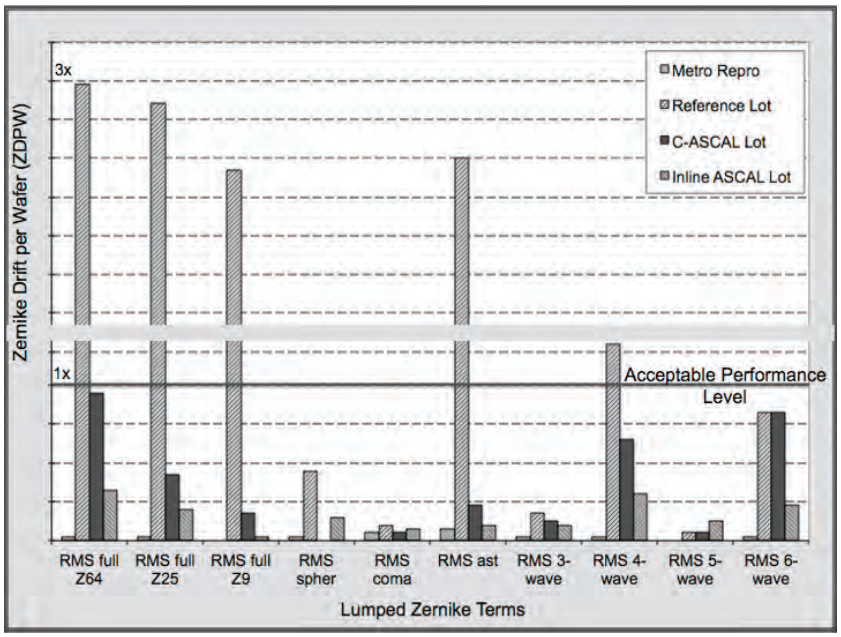

Figure 13. Experimentally measured Wafer Drift for lens heating controls with FlexWave comparing Inline ASCAL, C-ASCAL and the baseline performance.

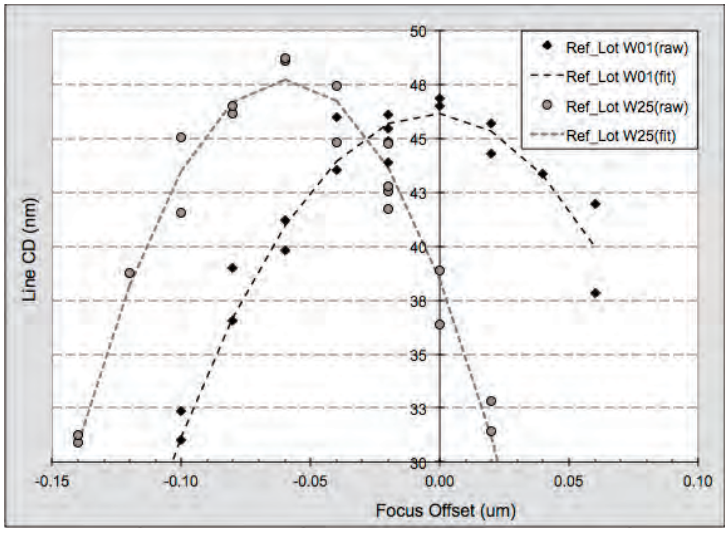

Figure 14. Experimentally measured best focus shift behavior for 200 nm pitch feature from baseline lens heating lot with no corrections applied.

45 nm lines on 104 nm pitch, 45 nm lines on 200 nm pitch, 95 nm lines on 300 nm pitch and 85 nm lines on 400 nm pitch. Note that the linear proximity curve through pitch applied to this test mask did not match the behavior of dipole 35x that was used in this experiment. However, the use of this dipole produced a measurable and controllable -60 nm of focus shift for the features of interest. It was observed that the 200 nm pitch demonstrated the largest best focus shift compared to the other three pitches described above, and thus the highest aberration sensitivity. Figure 14 shows experimental Bossung plot for the 45 nm (nominal) line on 200 nm pitch for the cold state (wafer 1) and the hot state (wafer 25). The best focus shift of -57 nm from this experiment matches well with the simulated value of -60 nm for the 200 nm pitch. One would expect that the degree of focus shift continues to increase from nested to isolated. However, the 300 and 400 nm pitches display half the observed shift due to larger CD values and flatter Bossung plots. Thus, the 200 nm pitch structure can be used to visualize the performance of c-ASCAL and inline ASCAL for controlling the through lot best focus shift. The left side of Figure 15 shows the fitted Bossung plots for the 200 nm pitch feature of the four lots being studied: 1.) Reference lot, 2.)No heating lot, 3.) c-ASCAL lot and 4.) Inline ASCAL lot. From Figure 15 the lens heating control lots (c-ASCAL and inline ASCAL) demonstrate no measurable shift in best focus from first to last wafer in the lot compared to the large shift observed for the reference lot. It is notable that the c-ASCAL and inline ASCAL fitted Bossung plots for wafer 25 show a small CD difference of 2 nm from the reference lot and a slightly more narrowed Bossung curve. These effects are still being investigated and are most probably due to small uncorrectable Zernike drifts at the hot state. Additionally, the lens heating performance across the four different lots and four pitches of interest can be summarized and compared against simulated values on the right side of Figure 15. Here it is shown that FlexWave driven by c-ASCAL or inline ASCAL are comparable in controlling the best focus drift through the lot for all four pitches. It is observed that both controllers compare well with the no heating condition lot where only a small subset of fields were exposed to provide a non-lens heating reference case.

3.4 Controlling CD Thru Slit Signatures

In addition to a simple offset value as described above, the lens heating profile across the slit can create significant amounts of higher order field effects,[17] which are typically described by a tilt (Zx_1) for odd Zernikes and curvatures (Zx_2) for the dominant even Zernikes. Higher orders beyond tilt and curvature are possible, i.e. 3^{rd} order for odd Zernikes and 4^{th} order for even Zernikes, but are typically much smaller effects than the first and second order field effects. We both experimentally studied and simulated the CD through slit behavior of a NTD printed 110 nm contact hole on a 250 nm pitch with a staggered orientation. The illumination used to print

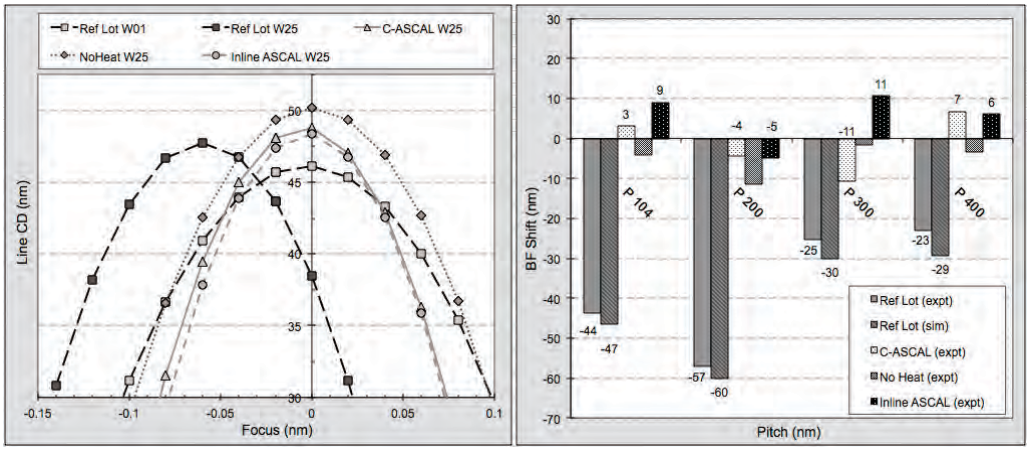

Figure 15. Left plot shows the fitted Bossung curves for the focus sensitive 200 nm pitch feature for all four lens heating lots. The right plot summarizes the best focus shift of all four pitches of the various lens heating lots including the experimentally measured and simulated baseline lot (no corrections applied).

this contact hole was the SMO pupil #1 with the high transmission reticle as described earlier. The primary aberration of concern was 4-foil (Z17_0) with a smaller amount of spherical (Z9_0) as shown in Figure 7. Tachyon LMC was used to simulate the contact hole CD through slit at the hot state for the following cases: baseline case (no corrections), the default lens manipulator (no Z17 control), ALC in rotated configuration (limited Z17 correction) and FlexWave. Figure 16 shows the various simulated lens manipulators with a experimental baseline, no corrections applied, for comparison. We have removed the DC offsets in Figure 16 to allow for a more direct comparison of only the CD through slit signature. The CD through slit fingerprint shows a maximum at the center of the slit and reduces sharply toward the edge of the slit. This behavior follows from the expected heating profile of the lens. The experiment matches the simulated baseline case and the default manipulator. Additionally, the simulated ALC response in the rotated configuration can remove about half of the CD through pitch signature which agrees with the previous mitigation discussion as measured Zernike values, specifically Z17. Lastly, FlexWave with its expanded dynamic range and full resolution of Zernike correction is predicted in these simulations to produce a very flat (less than 0.5 nm) CD through pitch signature at the hot state (wafer 25).

During the same experimental FlexWave work described above for Zernike drifts through lot and drifts per wafer, we also examined the performance of controlling the CD variation through the slit as a function of lens heating. The feature used to measure this effect was again the 45 nm lines on 200 nm pitch as used in the best focus shift discussion. The same four lens heating lots exposed on an immersion scanner with a FlexWave system were used: 1.) Baseline reference lot (no heating correction), 2.) c-ASCAL driven FlexWave with feed forward corrections, 3.) Inline ASCAL driven FlexWave with feed forward corrections, and 4.) No heating lot (with a small subset of dies exposed per wafer). Figure 17 shows the change in CD through slit from cold-to-hot state for these four lens heating lots. The reference lot shows a significant cold-to-hot CD thru slit difference of approximately 6 nm on the left side of the slit. The right side of the slit shows a linear behavior that can be traced to a small focus trend at cold state to dip slightly negative on the right most edge of the slit. Comparing the c-ASCAL, inline ASCAL to the no heating and baseline lots shows very reasonable performance in flattening the CD variation through slit. Thus FlexWave driven by either c-ASCAL or inline ASCAL demonstrates excellent capability to remove lens heating induced CD deviations through the exposure slit.

3.5 Controlling Image Placement Errors

In section 2.5, the importance of odd Zernike orders and their strong effect on image placement errors was described as compared to the larger magnitude but lower sensitivity even order Zernike terms. Thus, the lens heating induced odd Zernikes have been shown to significantly impact isolated-to-dense pattern placement errors through the slit. The large image placement sensitivity observed for (Z7_1) coma sensitive interlaced coarse and fine pattern overlay structures provides a convenient method for assessing the impact and the mitigation

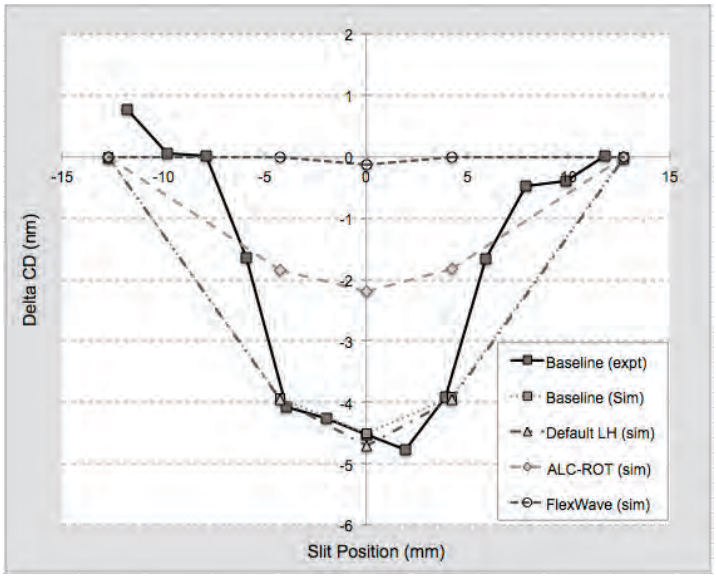

Figure 16. Experimentally measured contact hole CD through the exposure slit at the hot state (wafer 25) for the baseline case. Simulated CD through slit performance for baseline case, default controller, ALC-rotated and FlexWave.

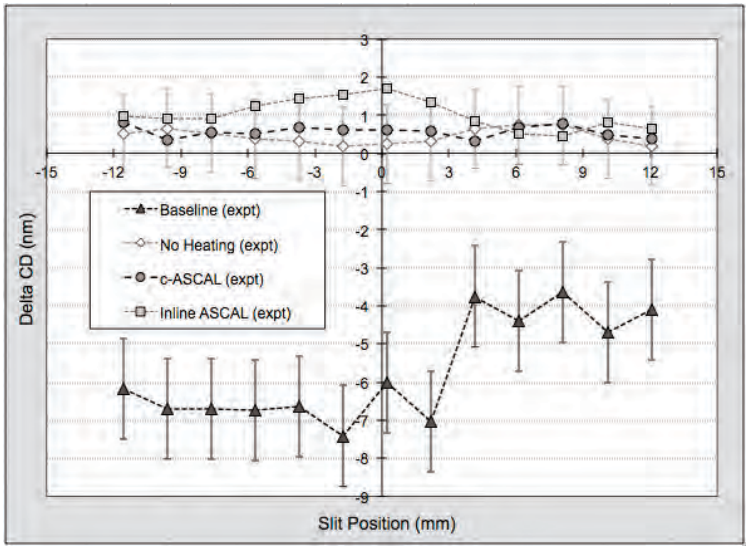

Figure 17. Experimentally measured change in CD for a 45 nm line on 200 nm pitch at the hot state (wafer 25) through the exposure slit. The performance of the four lens heating lots are compared: baseline condition, no heating condition, c-ASCAL and inline ASCAL corrected.

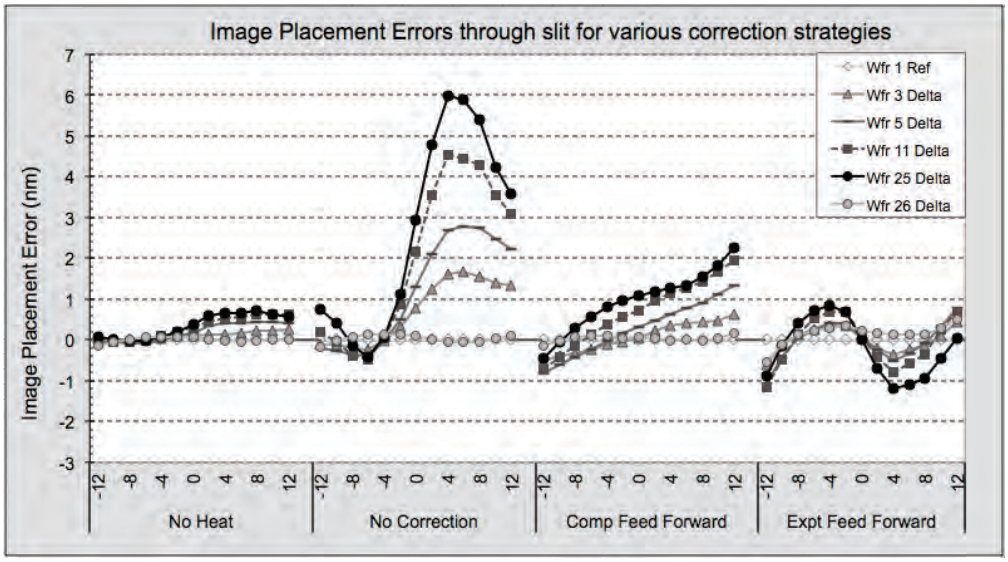

Figure 18. Experimentally measured image placement error through slit for the four various lens heating lots. The cold-to-hot difference is plotted as the lot progresses from wafer 1 to 25 with a lot transition (wafer 26).

of through lot and through slit lens heating effects. Using the same dipole 35x illumination with the high transmission reticle, we can judge the effectiveness of lens heating control with the FlexWave manipulator, based on both experimental and computational calibration. Additionally, the lens heating performance when transitioning to the next lot was assessed by exposing the 25 wafer lot followed by a single wafer lot (the 26^{th} wafer). Figure 18 shows image placement error (DX) as a function of slit position for wafers 1-25 & wafer 26 (new lot) for the same four lens heating lots. In this Figure 18, the overlay measurements are plotted the as the difference from the cold state (wafer 1) in each of the four lots. The baseline lot demonstrates a significant (> 6 nm) through slit image placement error through the slit at the hot state (wafer 25). The no heating case, where only a small subset of dies are exposed per wafer, shows < 1 nm deviation through the exposure slit for all 25 wafers in the lot. The c-ASCAL and inline ASCAL lots demonstrate a significant improvement over the baseline case, but still some measurable through slit effects for image placement errors. The c-ASCAL lot is shown to achieve < 2.5 nm through slit image placement error at the hot state. Inline ASCAL performs slightly better in this test with the hot state showing < 2 nm image placement error through slit. Transitioning directly to the next lot, wafer 26, shows that the lens heating effect from the prior lot is well corrected by the exposure tool's lot control scheme for all four runs. From the data in Figure 18, it is shown that both c-ASCAL and inline ASCAL using FlexWave are highly effective in suppressing the coma sensitive image placement error through the exposure slit as the lens heats during an exposure lot . Since we have previously shown that odd order Zernike terms have less sensitivity to pupil shape and fill fraction, the use of lens heating mitigation strategies to control these types of image placement errors for NTD processes is important to overlay budgets.

4. CONCLUSION

This investigation demonstrates that high transmission reticles, required by NTD processes, in combination with both free-form and standard pupils show significant lens heating effects during the lot exposure on a high throughput immersion scanner even at typical process doses. First, we showed that the Zernike drift term scales linearly with transmission value, as expected; however, comparing the split bright field/ dark field reticle , the coma aberration (Z7_0) is quite sensitive to the tone of the reticle. Although the pupil fill has been previously assumed to be sensitive to lens heating, we show that over a large range of pupil fill variations of rotationally symmetric quasar illuminators, a negligible difference in even and odd order Zernike drifts is observed. Both experimental and simulation of different free form pupils with the same high transmission reticle clearly demonstrates that pupil shape has a strong impact on lens heating, impacting both even and odd order Zernike amplitudes. Although the odd order terms, associated with variations of image placement or overlay, are much smaller than the even order Zernike terms, associated with CD and focus shifts, the odd order terms can show significant sensitivity thru the slit to features on the wafer. The rise and fall rates of the Zernike amplitudes suggest that the naive assumption that kinetic rate behavior scales with the Zernike order, does not alway hold.

The simulation studies presented here for SMO pupils and high transmission reticles show the experimental and computational lens heating calibration closely matches to within measurement error of the Zernike drift per lot. The control performance with ALC is shown to be superior to one without, which is further exceeded by applying the FlexWave manipulator. The simulated feed forward corrections used by the advanced lens controller are shown to significantly reduce the lens heating aberration drift per lot as compared to the default lens manipulator. Flexwave Zernike amplitude simulations are predicted to further reduce the lens heating drifts in comparison to the ALC controller. Experimental evaluation of FlexWave with a dipole 35x illuminator with the same high transmission reticle, shows that both lens heating control based on both experimental and computational calibration provide an acceptable level of aberration control.

Examination of through pitch focus drift from cold to hot state during a reference heating lot exposure shows significant shifts of the Bossung curves, resulting in approximately 60 nm of best focus shift. After enabling FlexWave, the focus drifts are observed to be negligible at the measured pitches and are comparable to the no heating lot. Lens heating effects on the reference lot are observed to cause large CD shifts from cold to hot state and have significant variation through the slit. Simulations of CD deviation through the exposure slit suggest that default lens manipulator can suppress these CD shifts, while ALC and FlexWave can further reduce the CD shift. While ALC and FlexWave simulations show a reduction the CD shifts by half and complete reduction, respectively. Experiments confirmed the CD drift was completely suppressed at the hot lens state to the level equivalent to the cold lens state with the lens heating control by the FlexWave manipulator.

Overall we have shown that while lens heating effects of NTD high transmission reticles are not insignificant, lens heating mitigations solutions are quite effective in suppressing them. Additionally, we have showed that predictive capability of the LHM and LMC computation engine to both estimate the lithographic impact of lens heating and providing effective calibration input to the controllers of the ALC and Flexwave lens heating mitigation systems.

ACKNOWLEDGEMENTS

The authors would like to acknowledge the important contribution of the following colleagues. Key contributors from the IBM team: Chris Robinson, Wally Carpenter, Ray Goss and IBM Fab Operations team. The ASML BRION contributors included: Wenjin Huang, Martin Snadjr, Hua Cao. The ASML Veldhoven team contributors were: Arjan Verhappen, Angelique Nachtwein, Konstantinos Kontagiannos, Patrick Thomassen, Peter van Kruisbergen, Jan Baselmans, Laurens de Winter. Our local ASML Albany team contributors were: James Waddell, Jerry Woods, Kevin Burr and Burnell McKenzie. Thanks to all of these team members for your important contributions and support of this work.

REFERENCES

[1] T. Brunner and C. Fonseca, Optimum tone for various feature types: positive versus negative, Proc. SPIE 4345, 30 (2001).

[2] J. Bekeart et al., Comparing positive and negative tone development process for printing the metal and contact layers of the 32- and 22-nm nodes, J. Micro/Nanolith. MEMS MOEMS 9, 043007 (2010).

[3] T. A. Brunner, Impact of lens aberrations on optical lithography, IBM Journal of Research and Development 41, 57 (1997).

[4] J. Cantone et al., "Negative-tone imaging (NTI) at the 22 nm node: process and material development, " Proc. SPIE 7972, 79720M (2011).

[5] B. Cheng et al. Improve the image control by correcting the lens heating focus drift, Proc. of SPIE 4000, 818 (2000).

[6] G. Landie et al., Fundamental Investigation of Negative Tone Development (NTD) for the 22nm node (and beyond), Proc. SPIE 7972, 797206 (2011).

[7] G. H. Ho et al., Lens Heating Induced Focus Drift of i-line Step & Scan: Correction and Control in a Manufacturing Environment, Proc. SPIE 4344, 289 (2001).

[8] D. F. Huang et al., Investigation of Lens FPD and LH Effect on CD Control of Lithography Process, Proc. SPIE 3892, 282 (1999).

[9] C. Progler and A. Wong, Zernike Coefficients: Are they really enough?, Proc. SPIE 4000, 40 (2000).

[10] V. N. Mahajan, Zernike polynomials and aberration balancing," Proc. SPIE 5173, 1 (2003).

[11] P. Liu et al., A computational method for optimal application specific lens control in microlithography, Proc. SPIE 7640, 76400M (2010).

[12] J. Bekaert et al., Characterization and control of dynamical lens heatings effects under high volume manufacturing conditions, Proc. SPIE 7973, 79730V (2011).

[13] J. Bekaert et al., Experimental verification of source-mask optimization and freeform illumination for 22-nm node staticrandom access memory cells, J. Micro/Nanolith. MEMS MOEMS 10(1), 013008 (JanMar 2011).

[14] J. Lim et al., Advanced Scanner Matching using Freeform Source and Lens Manipulators, Proc. SPIE 7973, 79732A (2011).

[15] Y. Ohmura et al., An aberration control of projection optics for multi-patterning Lithography, Proc. SPIE 7973, 79730W (2011).

[16] Y. Cui, Fine Tune Lens Heating Induced Focus Drift with Different Process and Illumination Settings, Proc. SPIE 4348, 1369 (2001).

[17] P. Evanschitzky et al., Compensation of mask induced aberrations by projector wavefront control, Proc. SPIE 7973, 797329 (2011).